5A.2 DIURNAL CYCLES OF CLOUD FORCING OF THE SURFACE RADIATION BUDGET

Pamela E. Mlynczak
Science Applications International Corporation, Hampton, VA

G. Louis Smith
National Institute of Aerospace, Hampton, VA

Paul W. Stackhouse, Jr.
NASA Langley Research Center, Hampton, VA

J. Colleen Mikovitz
Analytical Services and Materials Inc., Hampton, VA

1. INTRODUCTION

Sunlight provides the energy which drives the circulations of the atmosphere and oceans, thus determining our weather and climate. Most of the solar radiation that is absorbed by the Earth is absorbed at the surface, with a much smaller amount absorbed in the atmosphere. This radiation that is absorbed at the surface heats the surface and provides energy which is transferred to the atmosphere as sensible and latent heat. In addition, the surface heats the atmosphere by upward longwave radiation and is in turn heated by downward longwave radiation from the atmosphere. The radiation at the surface is fundamental to the energy and water cycles on our planet. For this reason, as part of the Global Energy and Water Experiment (GEWEX), the Langley Research Center of NASA has developed a Surface Radiation Budget (SRB) data set based on satellite observations which provides radiation components at the surface over the globe.

Clouds are the strongest modulators of radiation at the surface and at the "top of the atmosphere." The dynamics of clouds, their formation and dissipation, is a difficult problem which lies at the heart of our understanding of weather and climate. Information about the interaction of clouds with the energetics of the surface will be useful. The incorporation of clouds in circulation models is the major problem in their development, thus an observational knowledge of cloud effects on surface radiation to modify the energetics of the surface will be useful in that area of research.

Mlynczak et al. (2006) used the NASA/GEWEX SRB data set to investigate the diurnal cycle of surface radiation components. The SRB data set includes the radiation components at the surface for the clear sky case, i.e. in the absence of clouds, as well as the values for the clouds present, so that the effects of clouds on the surface radiation can be easily computed. The present paper uses the SRB data set to quantify the diurnal cycle of cloud forcing of the surface radiation components. The diurnal cycle of surface radiation is greatest in summer, when the insolation is greatest, and over land, where the surface heating during the day is large, in contrast to over the ocean, whose tremendous heat capacity results in very little change of temperature during the day. This study focuses on the diurnal cycle for a climatological July, because the diurnal cycle is greatest in this month in the Northern Hemisphere, where most of the Earth's land mass is located.

Corresponding author address:
Pamela E. Mlynczak, SAIC, 1 Enterprise Pkwy., Suite 300, Hampton, VA 23666.
Email: p.e.mlynczak@larc.nasa.gov

2. DATA SET

The NASA/GEWEX Surface Radiation Budget (SRB) data set was developed in response to the need for such information by the climate research community (Suttles and Ohring, 1986). The data set used in the present study for longwave flux is SRB Release 2.5 and for shortwave flux is Release 2.7. Gupta et al. (2004) and Cox et al. (2006) describe the data set, which has a number of improvements over the earlier data set and covers the period from July 1983 through June 2005. The improvements include updated cloud parameters, especially near the Sun-glint. The SRB data set includes the fluxes at the surface of insolation (shortwave radiation down, SWD), the reflected solar radiation (shortwave up, SWU), the radiation emitted by the atmosphere (longwave down, LWD), and the radiation emitted by the surface (longwave up, LWU). In addition, the shortwave net (SWN) and longwave net (LWN), which are the differences of the upward and

downward components, and the total net (TN), which is the sum of SWN and LWN, can therefore be calculated. This data set gives global coverage with a quasi-equal angle grid approximating one-degree resolution at the Equator, and the fields are archived for every three hours starting with midnight at Greenwich. The radiation budget terms (SWD, LWU, etc.) are computed for eight times per day based on the meteorology at GMT = 0600, 1200, 1800 and 2400 hours. These meteorological values are interpolated to get eight times per day, or every three hours in the SRB data set. Temperature and humidity profiles are taken from the Goddard Earth Observing System-4 (GEOS-4) reanalysis project at six-hourly intervals starting at midnight GMT. Cloud properties are derived from the International Satellite Cloud Climatology Project DX data (Rossow and Schiffer, 1991). For less than 50% cloud cover, the skin temperature from ISCCP is used for computing upward longwave flux LWU, where as for cloud cover greater than 50%, the surface temperature is taken from GEOS-4. Where ice or snow cover exceeds 80%, the ISCCP skin temperature is used. The ocean temperature is taken from the Reynolds' analysis once per week, and the diurnal cycle of ocean temperature is assumed to be negligible.

3. RESULTS

The diurnal cycles of surface radiation components for the all-sky case were investigated by Mlynczak et al. (2006). In order to examine the effects of clouds over all of the regions of the Earth quantitatively, it is useful to compute the diurnal-mean effects of clouds. This requires subtracting the clear-sky flux from the all-sky flux. Next, we define the magnitudes and shapes of the diurnal cycles, which is done well by use of principal component analysis.

3.1 Surface Radiation for Clear Sky

Figure 1a is a map of the downward shortwave flux at the surface for clear sky. The major determinants are the solar declination and latitude, which define the insolation at the top of the atmosphere.

Figure 1b shows the downward longwave radiation at the surface for clear sky. The strongest effect is latitude. Over most of the tropical regions, LWD is 350 to 400 W m^{-2}. Over the Southwest Pacific convergence zone and the areas around the monsoon regions of South Asia, LWD exceeds 400 W m^{-2}. The Sahara, Kalahari and Australian Deserts have low values compared to other regions at the same latitude, due to the low humidity over these areas. The Himalayan, Andes and Rocky Mountains also have low LWD due to the low absolute humidity of these regions and the reduced atmosphere above these regions.

3.2 Diurnal Mean Maps of Cloud Forcing

Figure 2a shows the diurnal mean of cloud forcing of downward shortwave flux at the surface for an average July. Clouds reflect and absorb solar radiation, so that they only decrease SWD. This decrease is less than 20 W m^{-2} over parts of the deserts of North Africa, South Africa, the Middle East and Australia, and less than 40 W m^{-2} over the subsidence regions of the tropical Atlantic and Pacific Oceans. Also, during July the convection over South America has moved from the Amazon Basin northward to Venezuela. Over most of the tropical and southern oceans, the effect of clouds is to reduce SWD by 20 to 40 W m^{-2}, except south of the Roaring Forties, where the effect of clouds is less than a 20 W m^{-2} reduction of SWD, as the insolation decreases with latitude in the winter hemisphere. The Intertropical Convergence Zone is marked by clouds reducing SWD by 80 to 140 W m^{-2}. Over the oceans north of 30^{o}N, clouds reduce SWD by more than 80 W m^{-2}, and the reduction exceeds 160 W m^{-2} in mid-ocean over both the Atlantic and Pacific Oceans. Clouds diminish SWD over high latitudes of North America and Eurasia by 80 to 100 W m^{-2}. Over the subcontinent of India, Southeast Asia and much of China, the cloud effect exceeds 100 W m^{-2}, with peaks over Myanmar and the Bay of Bengal. The monsoon is active over these regions during July.

Clouds increase downward longwave radiation at the surface (LWD) by an amount depending on the cloud fraction and the cloud base altitude. Figure 2b shows the increase of diurnal-mean LWD for July. Over the desert region where the paucity of clouds causes a minor decrease of SWD, the increase of LWD is less than 20 W m^{-2}. Over most of the Southern Ocean, clouds increase LWD by 40 to 60 W m^{-2}. For much of the northern parts of the Pacific, Atlantic and into the Arctic Ocean, clouds increase LWD by 40 to 60 W m^{-2}. Clouds over Tibet and the surrounding regions also increase LWD by 40 to 70 W m^{-2}. For most of the remaining latitudes between 30^{o}S and 60^{o}N, clouds increase LWD by 20 to 40 W m^{-2}.

The upward shortwave flux is simply the SWD times the surface albedo and is not discussed here. The upward longwave flux depends only on

the surface temperature and emissivity, and no attempt is made to account for temperature change due to the presence or absence of clouds. Consequently, there is no cloud forcing of upward longwave flux.

3.3 Diurnal Cycles of Cloud Forcing over Land

Figure 3a shows diurnal cycles of downward shortwave radiation at the surface for five sites for the July average. For Colorado, the peak SWD is just before noon, due to the build-up of clouds during the day. Over Australia, there are few clouds, and so the SWD is symmetric about noon. Pennsylvania is near the same latitude as Colorado, but it has greater cloudiness, and the SWD is symmetric about noon, indicating little change of clouds during the day as a daily mean. Myanmar and the Ivory Coast are at low latitudes so that at the top of the atmosphere the insolation is large, but the monsoon is active during July, and clouds greatly reduce the SWD. Also, the maximum SWD is well after noon, indicating greater cloudiness in morning than in afternoon.

Figure 3b shows the cloud forcing of SWD for these regions. Colorado shows a reduction of SWD peaking at 250 W m^{-2} near 1400 hours. The Australian Desert shows a decrease in SWD of less than 50 W m^{-2}. Over Pennsylvania the decrease is about 240 W m^{-2} and is greatest near noon. The reduction of SWD over Myanmar exceeds 500 W m^{-2} and also peaks near noon.

The diurnal cycles of LWD for these five sites are shown by fig. 4a. All the sites except Myanmar show a cycle of heating during the day. LWD for the Ivory Coast ranges from a high of 425 W m^{-2} just before noon to a low of 390 W m^{-2} near sunrise. Colorado has a greater variation of LWD during the day, with a range of 315 to 370 W m^{-2} and a peak in the afternoon. The Australian Desert has a low LWD due to the low cloud amount and low humidity.

The cloud forcing of LWD is shown by fig. 4b and is an order of magnitude smaller than the cloud forcing for SWD. For Myanmar the maximum cloud forcing is only 22 W m^{-2}, compared to that for Colorado, where the cloud forcing of LWD goes from a minimum of 14 W m^{-2} at sunrise to 50 W m^{-2} at 1400 hours. Over Myanmar, the high humidity results in a large LWD in clear air, so that the effect of clouds on LWD is diminished. The Ivory Coast has a maximum around 1000 hours; diminishing clouds in the afternoon result in a reduction of the cloud forcing of LWD. In July, the monsoon is at a maximum over this region of West Africa.

In order to study the diurnal cycles of 44,000 regions which are required to cover the Earth using a quasi-equal area grid with one-degree resolution at the Equator, the method of principal component analysis is used, whereby the diurnal cycles are resolved into a sequence of dominant patterns. The diurnal cycles of downward longwave over the oceans are much smaller than over land, so that if the principal components were computed for the entire domain, including land and ocean, the land would dominate such that the diurnal cycles over the oceans would have little influence on the principal components. Also, the physical processes differ considerably for the diurnal cycles for radiation fluxes over land and ocean; thus it is useful to partition the domain into land and ocean so that the relation between the principal components and the physics can be discerned more easily.

In this application, the root-mean-square RMS of a quantity is the square root of the mean over the 24-hour cycle and over the geographic domain of the square of the quantity. The RMS of the diurnal cycle of cloud forcing of SWD over land is 66.7 W m^{-2}. The surface albedo is small over most land, so that the SWU is much smaller than the SWD. Table 1 lists the first three eigenvalues for the diurnal cycle of cloud forcing of SWD over land. The first principal component describes 96% of the variance of the diurnal cycle of cloud forcing of SWD. Figure 5 shows the principal components of the diurnal cycle of cloud forcing of downward shortwave radiation flux. The first principal component PC-1 has a half-sine shape with a maximum of 120 W m^{-2} near noon and a minimum of about -60 W m^{-2} at night. PC-1 is governed by the solar insolation through the clouds. Because the diurnal cycle is the difference of the instantaneous value from the diurnal average, the average of the diurnal cycle is zero. Also, the length of day varies with latitude, so PC-1 does not have a break in slope at a specific time of sunrise or sunset. The shape of PC-1 for cloud forcing of SWD is the same as for all-sky SWD (Mlynczak et al., 2006), but is smaller by a factor of about three.

Figure 6a shows the first empirical orthogonal function EOF-1 for diurnal forcing of SWD, which describes the geographical distribution corresponding to the time behavior of the first principal component. Because clouds reduce SWD, the cloud forcing of SWD is negative. PC-1 is taken to be positive during the day, and thus EOF-1 is negative. Results for cloud forcing over Antarctica and Greenland are not considered to be valid due to the problem of discriminating clouds

over snow and ice. The regions with the highest cloud forcing of SWD are from western India across Southeast Asia into southern China. In these regions EOF-1 varies from -2 to -3. Most of the Southern Hemisphere, the deserts of North Africa and the Middle East, and much of the United States and Northern Siberia have a diurnal cycle of cloud forcing of SWD less than 0.5 (absolute value). EOF-1 over the south coast of northwest Africa has a value of -1 to -2; the monsoon is active in this region during July. The convection region of South America is situated over Venezuela in July, where the EOF-1 values are from -1 to -2.

PC-2 (fig. 5) describes a lag or lead of the cloud forcing of SWD due to the increase and decrease of clouds during the day. EOF-2 is negative (positive) where clouds increase (decrease) in afternoon. This term accounts for only 2% of the power of the cloud forcing of SWD globally. Figure 6b shows that over most land, the magnitude of EOF-2 is much less than 1. However, in some regions, the magnitude of EOF-2 exceeds 3; in these regions, the effect of morning or afternoon clouds is important to the surface radiation budget. Over the western U. S. and Mexico, EOF-2 exceeds -3, indicating a strong afternoon cloud forcing of SWD and low morning effect. In such regions, there is strong insolation that is not reduced by clouds until afternoon, when convective activity creates heavy cloud cover. Near the southern coast of northwest Africa and over southern Asia, EOF-2 exceeds 4, indicating a strong morning cloud forcing but smaller in the afternoon. These regions have monsoons in July.

The third principal component of cloud forcing of SWD is a 2-wave (fig. 5) with minima near 0700 and 1700 hours, and PC-3 is due to the variation of length of day with latitude. EOF-3 (not shown) describes that variation. This third term accounts for 1.2% of the power of the diurnal cycle of cloud forcing of SWD.

The RMS of cloud forcing of downward longwave radiation flux LWD over land is 6.3 W m^{-2}, smaller than for SWD by a factor of 10. Table 2 shows that this term accounts for 71% of the power of cloud forcing of LWD. Figure 7 shows the principal components of cloud forcing of LWD. PC-1 approximates a sine wave with a range of 16 W m^{-2}, with a maximum at 1400 hours, lagging the insolation by two hours, and a minimum at 0500 hours. This term is due to the solar heating of the surface and atmosphere as they affect the clouds. Figure 8a is a map of EOF-1 for cloud forcing of LWD over land. Regions with positive values have maxima of LWD in the afternoon. Over much of Africa and Eurasia between 15^{o}N and 45^{o}N the map shows large afternoon cloud forcing of LWD. For southern parts of South America, Africa and Australia, the negative value of EOF-1 indicates that the maximum cloud forcing of LWD occurs in early morning.

The PC-2 for cloud forcing of LWD approximates a sine wave which is out of phase with PC-1 and has a range of 8 W m^{-2} (fig. 7). This term accounts for 16% of the variance of the diurnal cycle of cloud forcing of LWD. Figure 8b shows EOF-2. Much of North America and Eurasia has a negative EOF-2, which increases the LWD in the afternoon over these regions. Over the mountain states of the U. S. and over Mongolia the EOF-2 values are beyond –2. There are small regions with large negative values of EOF-2 over the Atlas Mountains and other locations across North Africa and Saudi Arabia, indicating a large afternoon increase of LWD due to cloud forcing. There are regions near the coast of equatorial Africa where EOF-2 has large positive values. Interestingly, the Ivory Coast is the only monsoon region which has a large EOF-2 for LWD, whereas several other monsoon regions have a large EOF-2 for SWD. For both SWD and LWD the large EOF–2 indicates much cloud in the morning relative to the afternoon.

Table 2 shows that the third term accounts for 5% of the variance of the diurnal cycle of LWD. PC-3 for cloud forcing of LWD is a 2-wave (fig. 7) with minima near sunrise and sunset. This term describes the variation of cloud forcing of LWD with latitude. EOF-3 (not shown) shows artifacts in addition to the latitudinal variation of length of day. The RMS of the third term is 1.4 W m^{-2}, which is at the noise level.

3.4 Diurnal Cycles of Cloud Forcing over Ocean

The diurnal cycle of cloud forcing of SWD over ocean has an RMS of 65.4, very close to that over land. Table 3 shows that the first principal component accounts for 97% of the variance of cloud forcing of SWD, again very near that over land. PC-1 for cloud forcing of SWD over ocean (fig. 9) describes the variation of insolation as weighted by the cloud effects. Figure 10 is a map of EOF-1. The greatest reduction of SWD is over the North Pacific and Atlantic Oceans and a small region in the Bay of Bengal. The Intertropical Convergence Zone appears to the north of the Equator in July, and the Southwest Pacific Convergence Zone straddles the Equator; these

regions have large cloud cover and thus appear here. The cloud forcing effects are very small over the Azores/Bermuda high pressure region and similar subsidence regions just south of the Equator. Here the EOF-1 values are small.

PC-2 for SWD cloud forcing is a 2-wave and is due to the variation of length of day with latitude, and EOF-2 (fig. 10b) describes this variation. PC-2 accounts for 1.8% of the variance for SWD cloud forcing. The third term expresses 0.5% of the variance, and PC-3 describes differences between morning and afternoon clouds. EOF-3 (not shown) shows both physical features and artifacts. These artifacts are believed to be due to the interpolation required to compute diurnal cycles at local solar times from data defined at GMT on three-hour intervals.

Whereas land heats up and transfers sensible heat to the atmosphere, the ocean surface temperature does not change appreciably. The diurnal cycle of LWD over the ocean is due to the absorption of solar radiation within the atmosphere, including the clouds. The diurnal cycle of cloud forcing of LWD over oceans has an RMS of 3.7 W m^{-2}, about half that over land. It was noted that over land the noise level is near 1.4 W m^{-2}, so more study is needed of cloud forcing of LWD over ocean.

4. CONCLUSIONS

The effects of clouds on the surface radiation budget have been evaluated using the NASA/GEWEX Surface Radiation Budget data set. The study was done for a climatological July, as the diurnal cycle is strongest in summer over land and most land is in the Northern Hemisphere.

The daily-mean shortwave flux at the surface is reduced by over 160 W m^{-2} over large expanses of the North Pacific and North Atlantic Oceans and over the region of South Asia which has an active monsoon. Over the North African and Middle-Eastern deserts and subsidence areas of the tropical Pacific and Atlantic Oceans and over much of the Southern Oceans, the reduction of downward shortwave flux is less than 40 W m^{-2}. Clouds increase the daily-mean downward longwave flux by up to 60 W m^{-2} over regions where large cloudiness causes much decrease in downward shortwave flux. The effect of clouds is less than 20 W m^{-2} over desert and ocean subsidence regions.

The diurnal cycles of cloud forcing of the components of surface radiation have been examined in terms of principal component analysis and EOF maps. The diurnal cycle of downward shortwave flux is driven primarily by the cycle of insolation at the top of the atmosphere together with a daily-mean cloud amount. Globally the mean cloud forcing of downward shortwave flux is 180 W m^{-2} near noon. The variation of cloud forcing of downward shortwave flux from morning to afternoon accounts for 2% of the change on a global basis, but is concentrated in regions where morning-afternoon cloud differences are important. In regions with monsoons and the eastern regions of the Pacific and Atlantic Oceans, the cloud forcing is highest in the mornings. The effect of clouds on the diurnal cycle of downward longwave flux is to change the flux during day by 16 W m^{-2} globally, with a complex geographic pattern which appears to be related to the climatological class of the region.

5. ACKNOWLEDGEMENTS

The authors gratefully acknowledge support by the Surface Radiation Budget Program from the NASA Office of Science through the Langley Research Center to Science Applications International Corporation, the National Institute of Aerospace, and Analytical Services and Materials, Inc. They also acknowledge the Atmospheric Sciences Data Center of Langley Research Center for access to the data set.

6. REFERENCES

Cox, S. J., P. W. Stackhouse, Jr., S. K. Gupta, J. C. Mikovitz, T. Zang, L. M. Hinkleman, M. Wild and A. Ohmura, 2006: The NASA/GEWEX Surface Radiation Budget Project: Overview and Analysis, *Proc. 12-th Conf. Atmos. Rad*., Madison, WI, Amer. Meteor. Soc., CD-ROM, 10.1.

Gupta, S. K., P. W. Stackhouse, S. J. Cox, J. C. Mikovitz and M. Chiacchio, 2004: The NASA/GEWEX Surface Radiation Budget Data Set, Preprint, *13th Conf. on Satellite Meteorology and Oceanography*, Norfolk, VA, Amer. Meteor. Soc., CD-ROM, P6.6.

Mlynczak, P. E., G. L. Smith, P. W. Stackhouse, Jr., S. K. Gupta, 2006: Diurnal cycles of the surface radiation budget data set, *18-th Conf. on Climate Var*., Atlanta, GA, Amer. Meteor. Soc., CD-ROM, P1.6.

Rossow, W. B. and R. A. Schiffer, 1991: ISCCP cloud data products, *Bull. Amer. Meteor. Soc.*, **72**, 2-20.

Smith, G. L. and D. Rutan, 2003: The diurnal cycle of outgoing longwave radiation from Earth

Radiation Budget Experiment measurements, *J. Atmos. Sci.*, **60**, 1529-1542.

Suttles, J. T. and G. Ohring, 1986: Surface radiation budget for climate applications, NASA Reference Publication 1169, NASA, Washington D.C., 132pp.

Table 1: Eigenvalues of diurnal cycle of cloud forcing of downward shortwave flux over land. RMS = 66.7 W m^{-2}

Order	Normalized eigenvalue	Physical cause
1	0.964	Insolation change during day
2	0.020	AM/PM cloud change
3	0.012	Change of length of day with latitude
Sum of first 3 terms	0.996	

Table 2: Eigenvalues of diurnal cycle of cloud forcing of downward longwave flux over land. RMS = 6.3 W m^{-2}

Order	Normalized eigenvalue	Physical cause
1	0.707	Heating of surface and atmosphere
2	0.157	AM/PM cloud change
3	0.053	Change of length of day with latitude; artifacts
Sum of first 3 terms	0.917	

Table 3: Eigenvalues of diurnal cycle of cloud forcing of downward shortwave flux over ocean. RMS = 65.4 W m^{-2}

Order	Normalized eigenvalue	Physical cause
1	0.974	Insolation change during day
2	0.018	Change of length of day with latitude
3	0.005	AM/PM cloud change; artifacts
Sum of first 3 terms	0.997	

a)

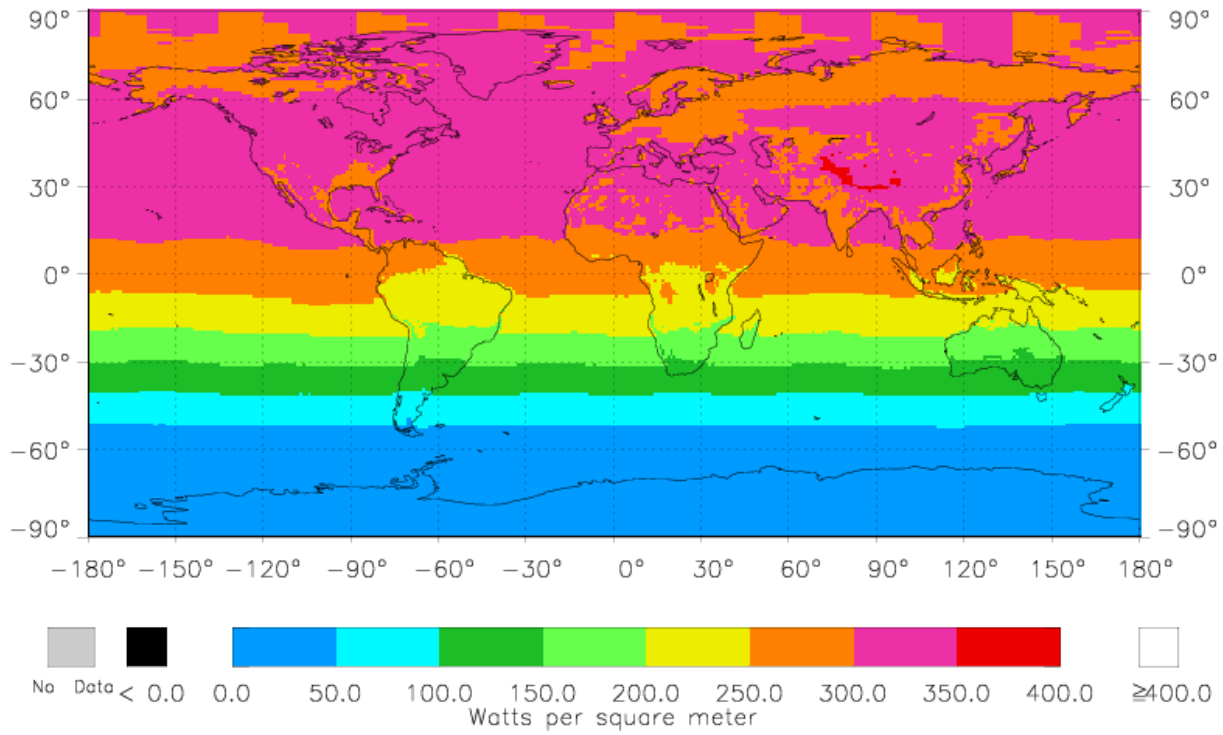

b)

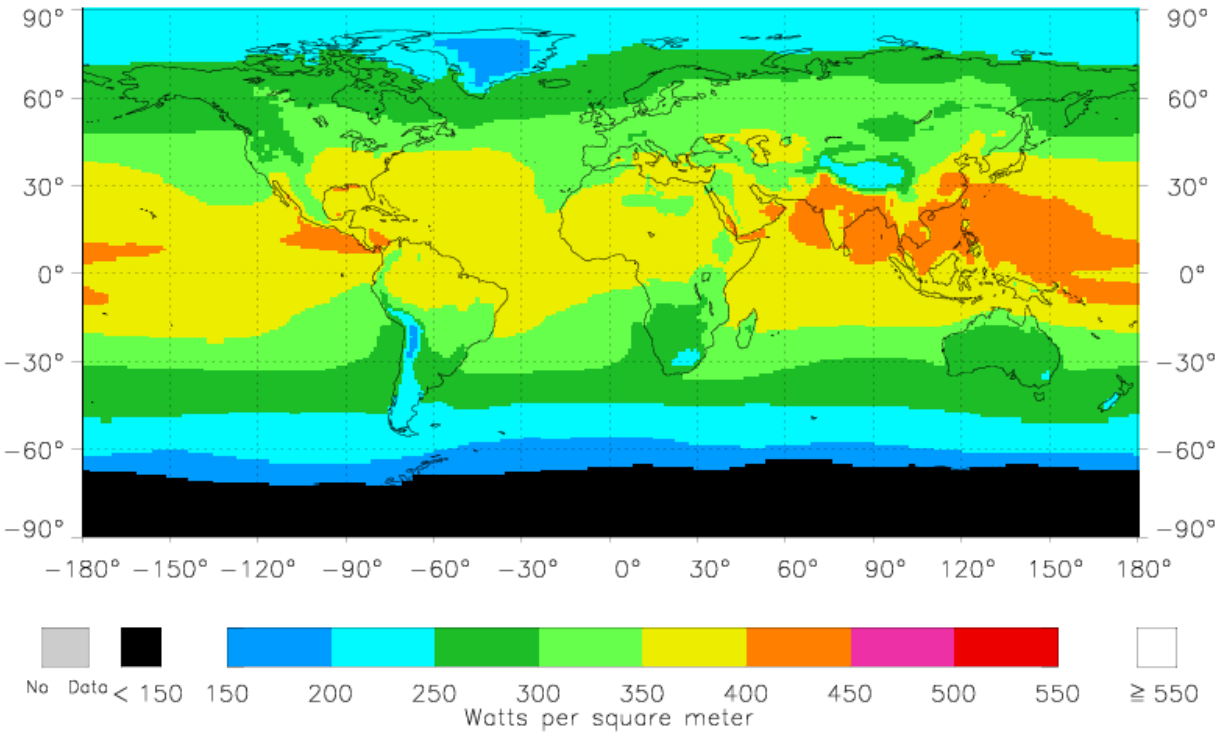

Figure 1. Diurnal mean maps of clear-sky downward fluxes, W m^{-2}.
a) downward shortwave flux, b) downward longwave flux.

a)

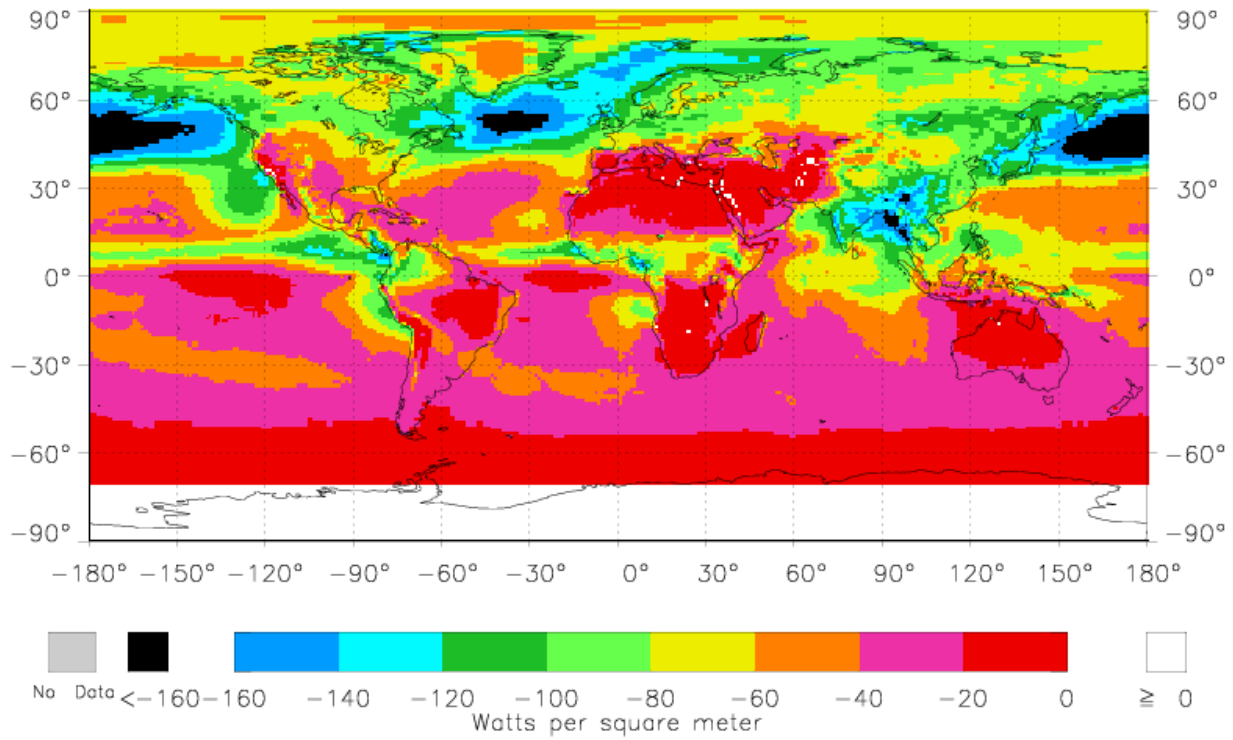

b)

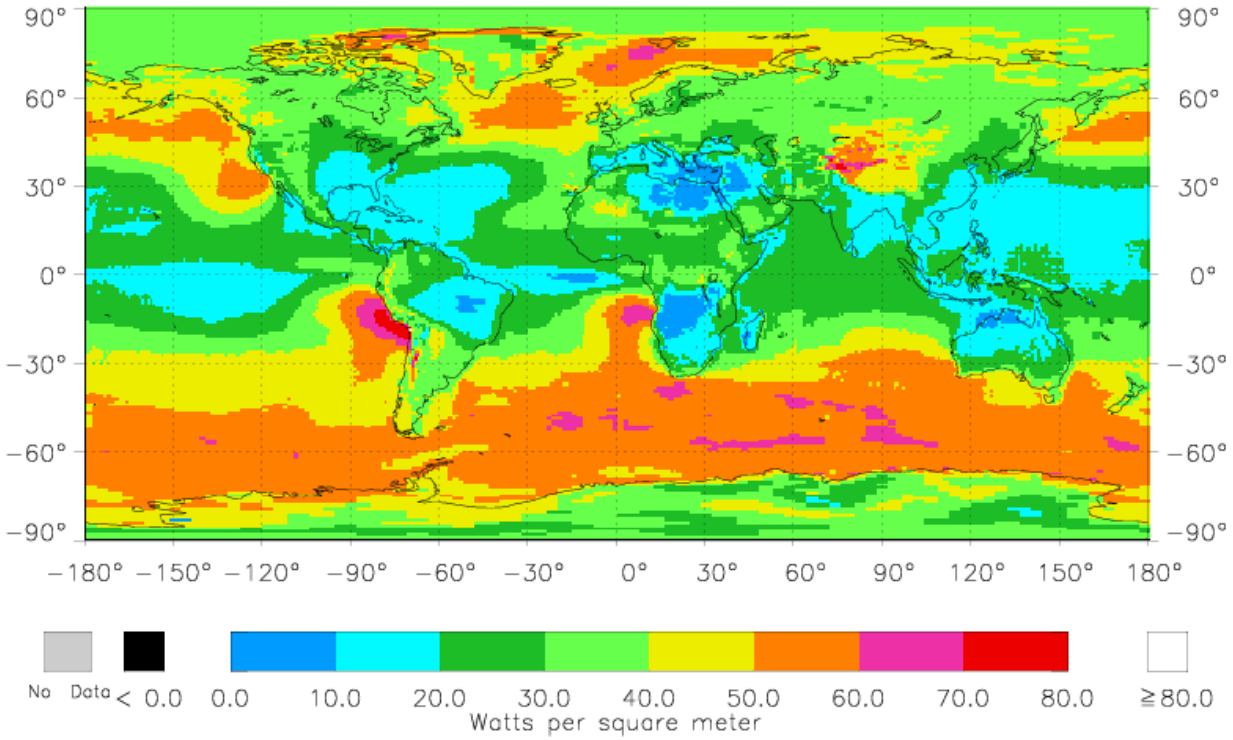

Figure 2. Diurnal mean maps of cloud forcing. a) downward shortwave flux, b) downward longwave flux.

a)

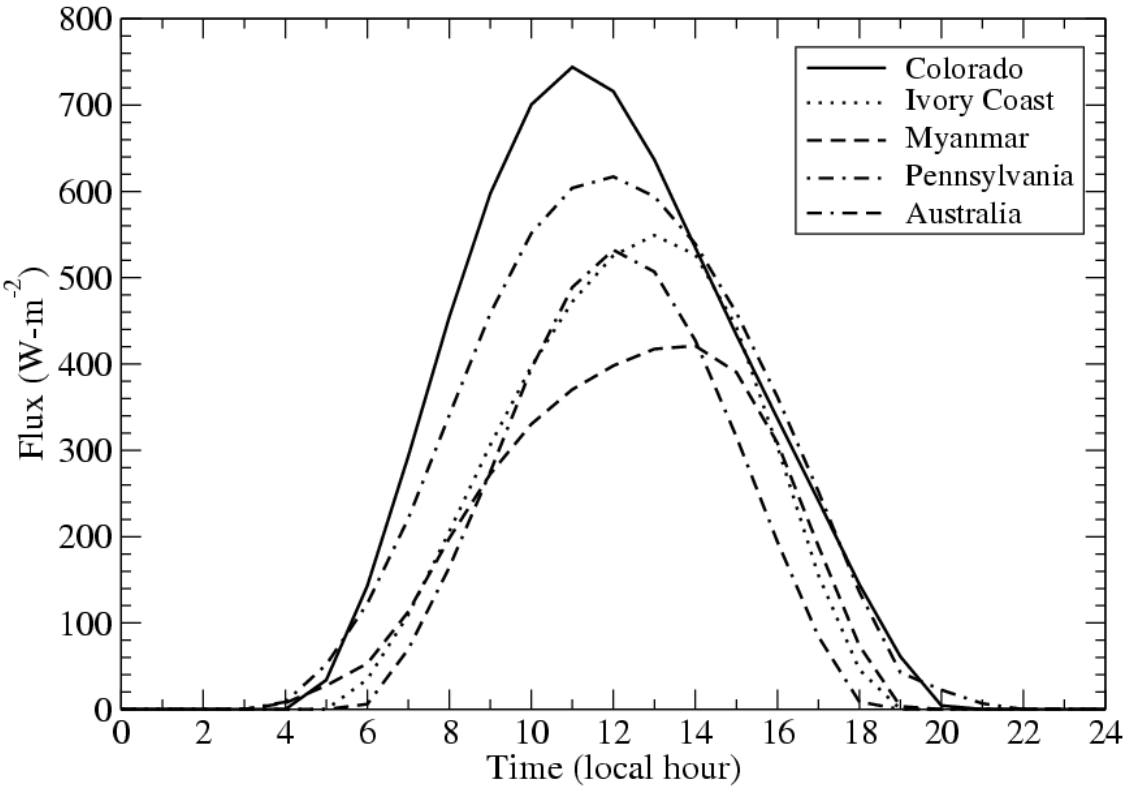

b)

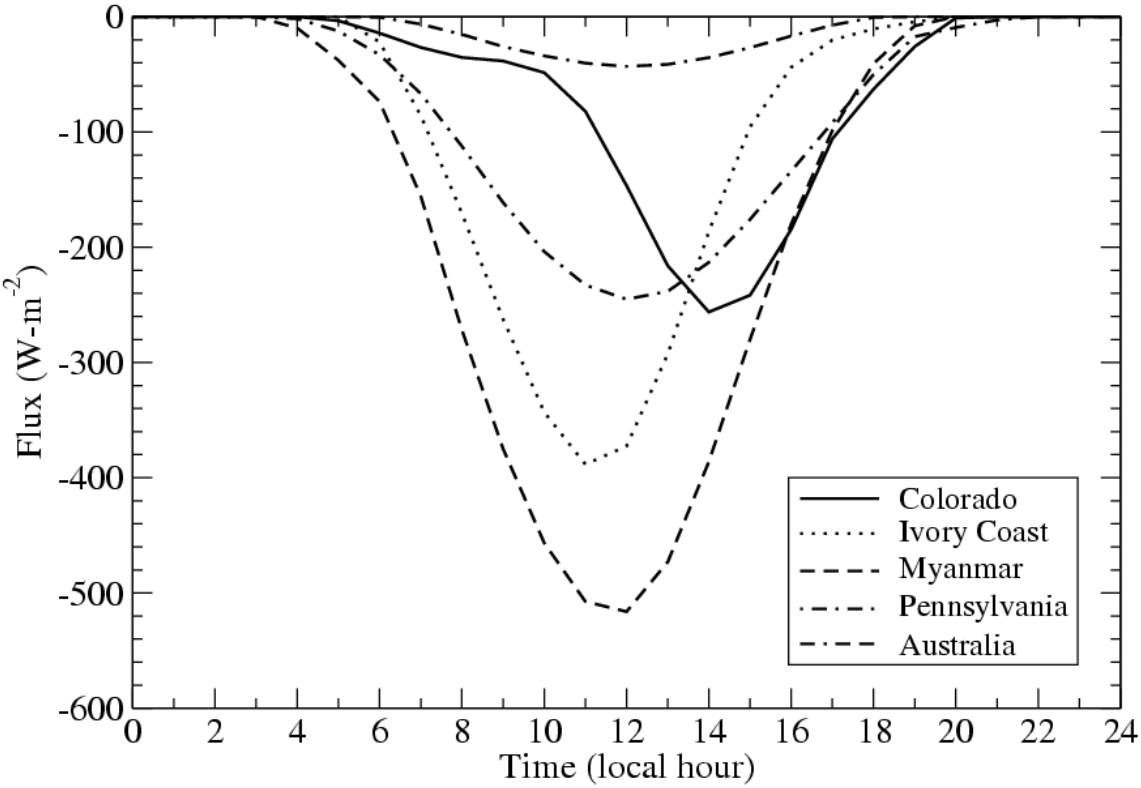

Figure 3. Downward shortwave flux at surface for five sites: Colorado, Ivory Coast, Myanmar, Pennsylvania, and Australian Desert, W m^{-2}, for a) all sky conditions, b) cloud forcing.

a)

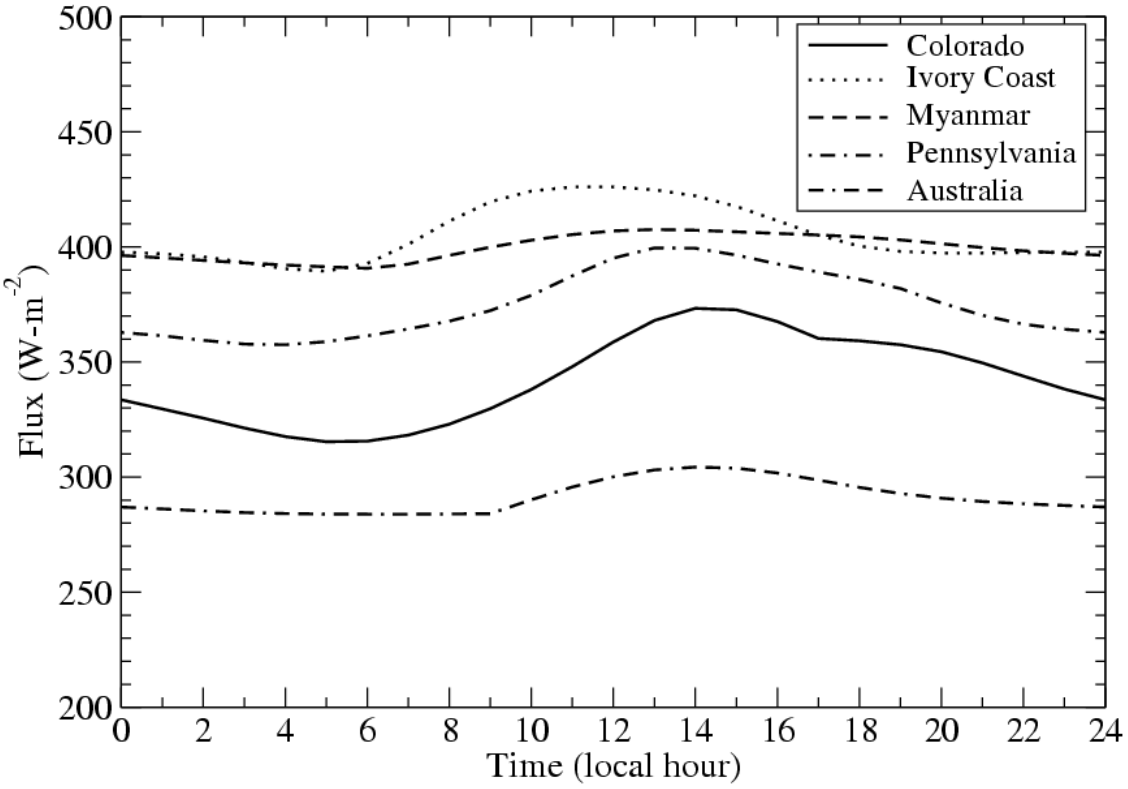

b)

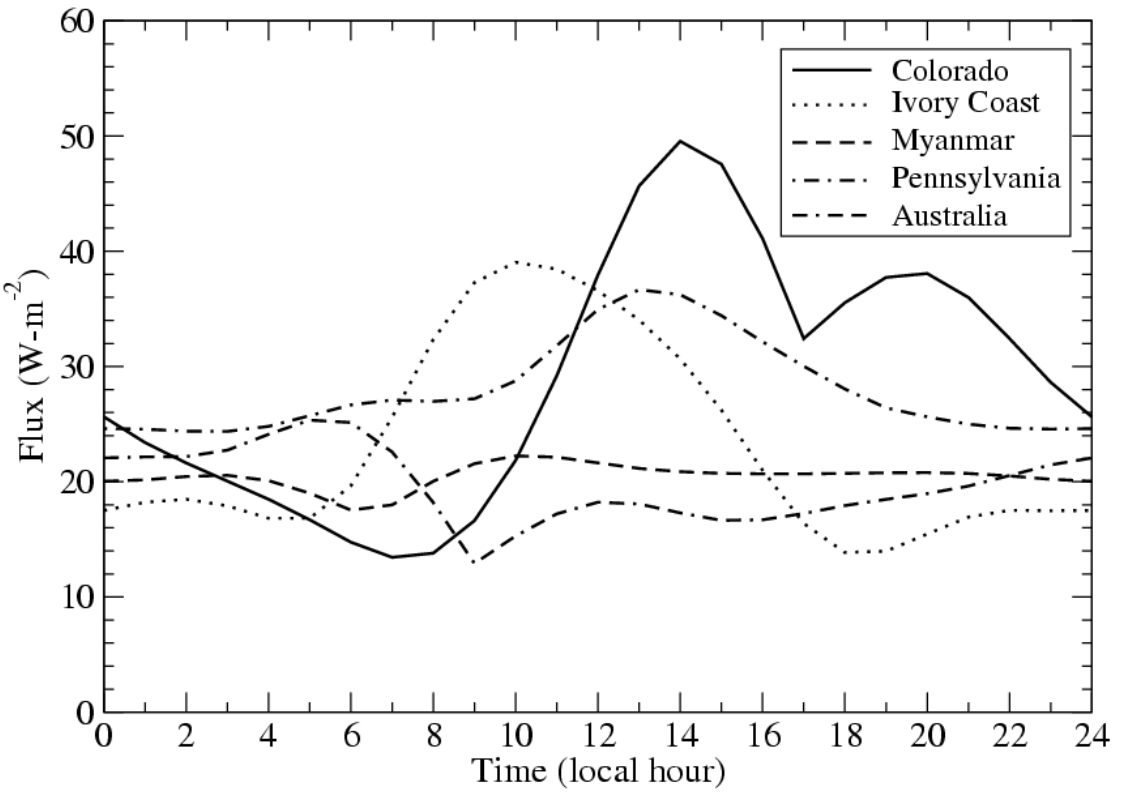

Figure 4. Downward longwave flux at surface for five sites: Colorado, Ivory Coast, Myanmar, Pennsylvania, and Australian Desert, W m^{-2}, for a) all sky conditions, b) cloud forcing.

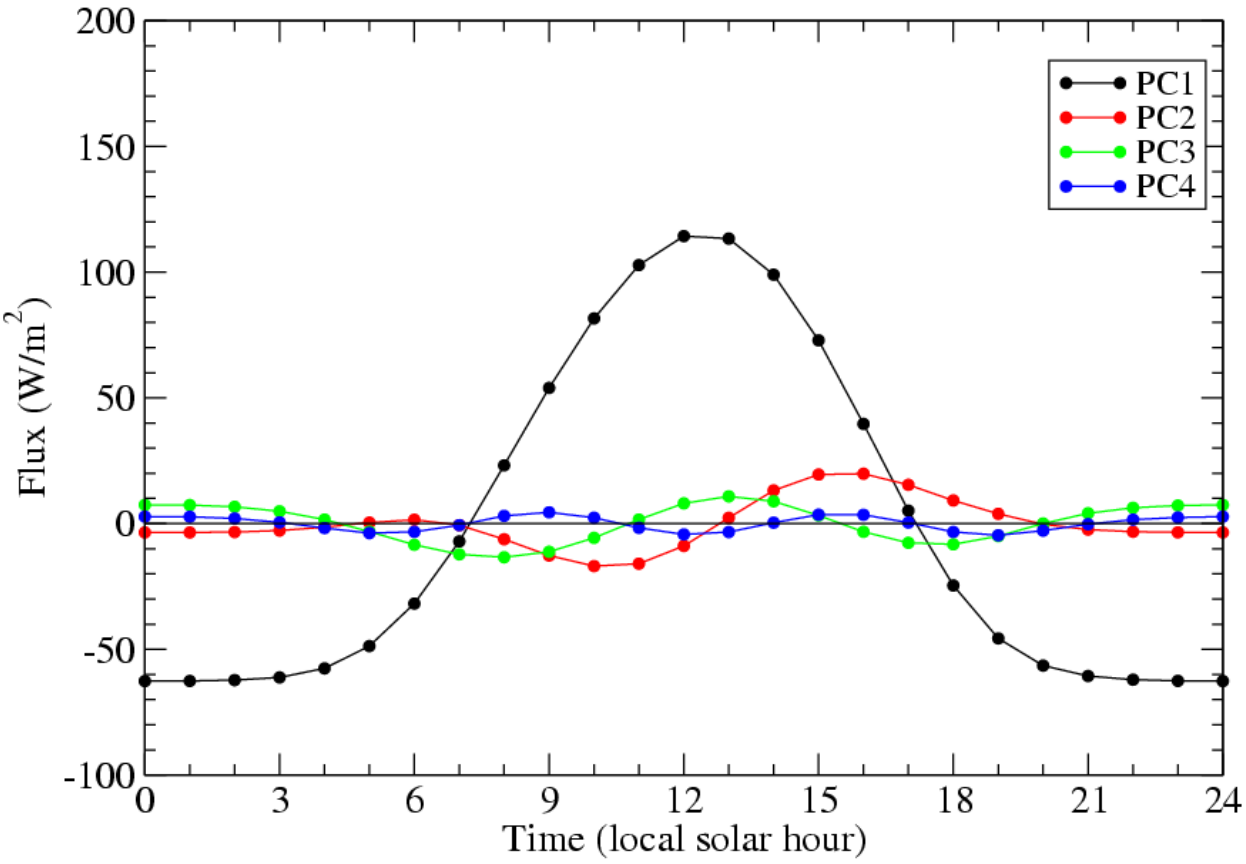

Figure 5. Principal components of diurnal cycles of cloud forcing of downward shortwave flux over land.

a)

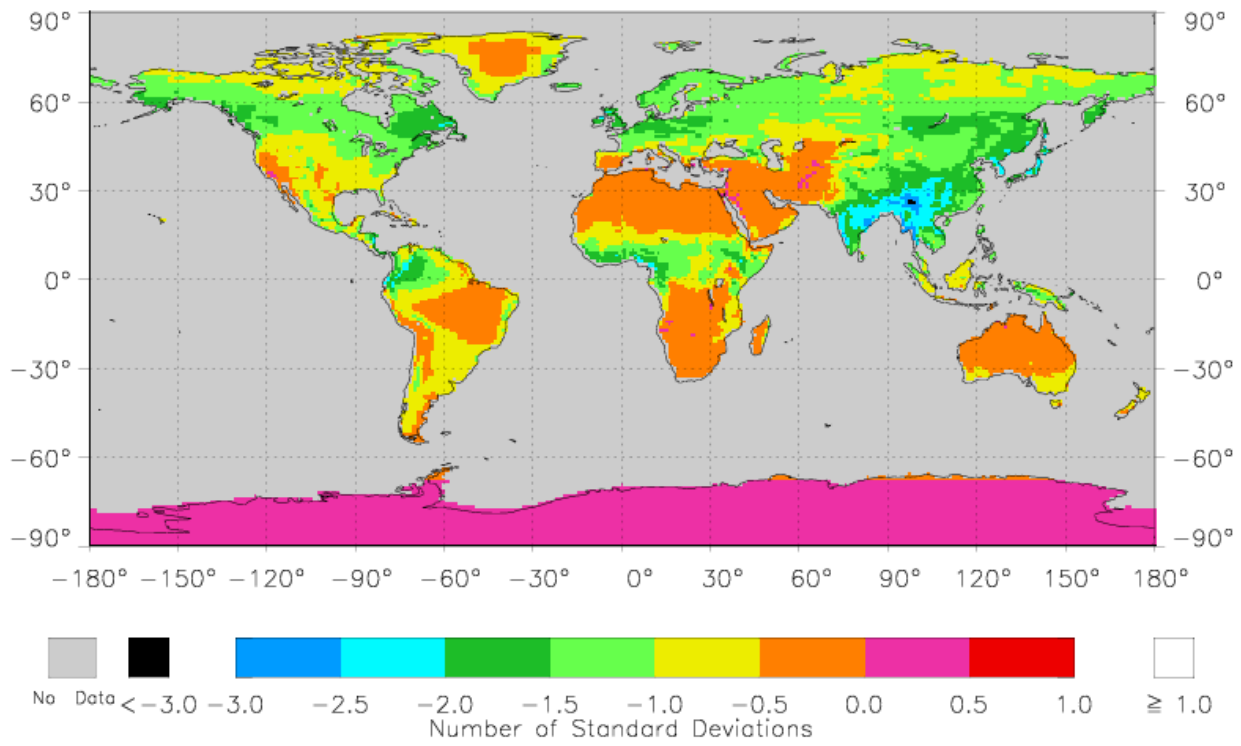

b)

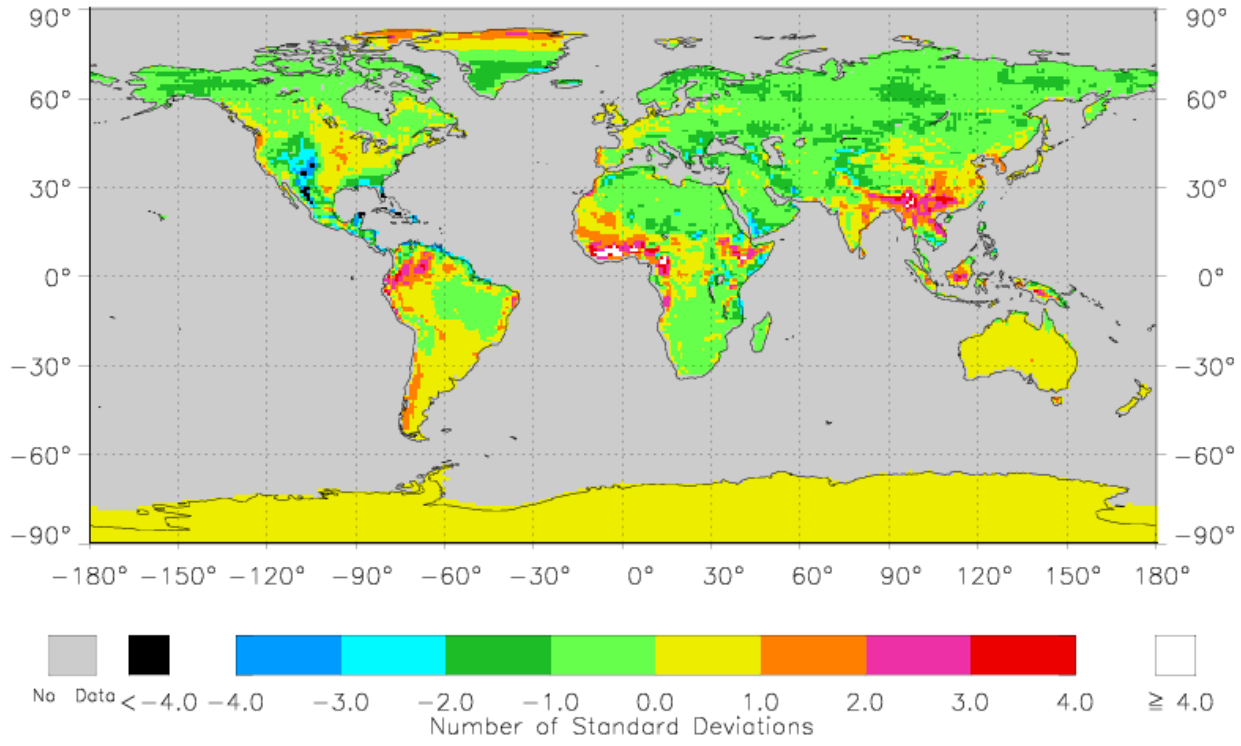

Figure 6. Map of empirical orthogonal functions of cloud forcing of downward shortwave flux over land for a) EOF-1 b) EOF-2.

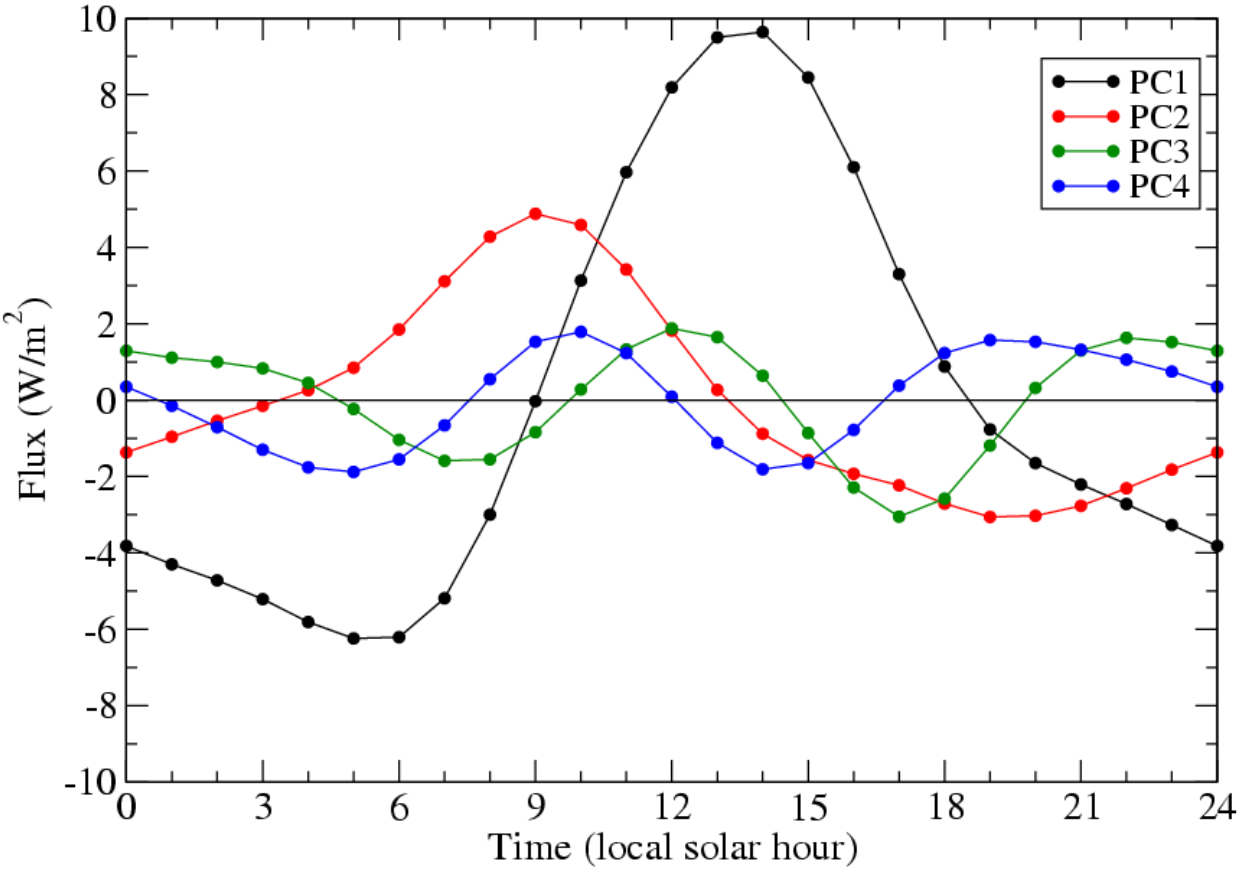

Figure 7. Principal components of diurnal cycles of cloud forcing of downward longwave flux over land.

a)

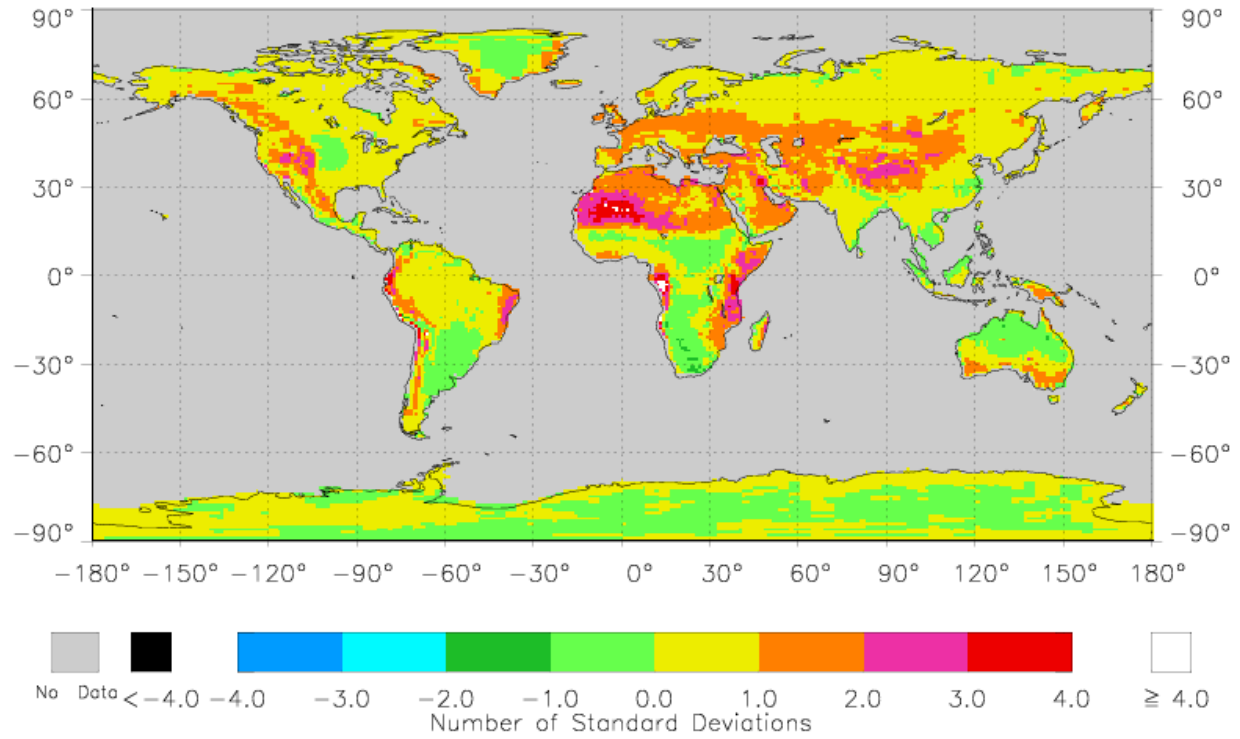

b)

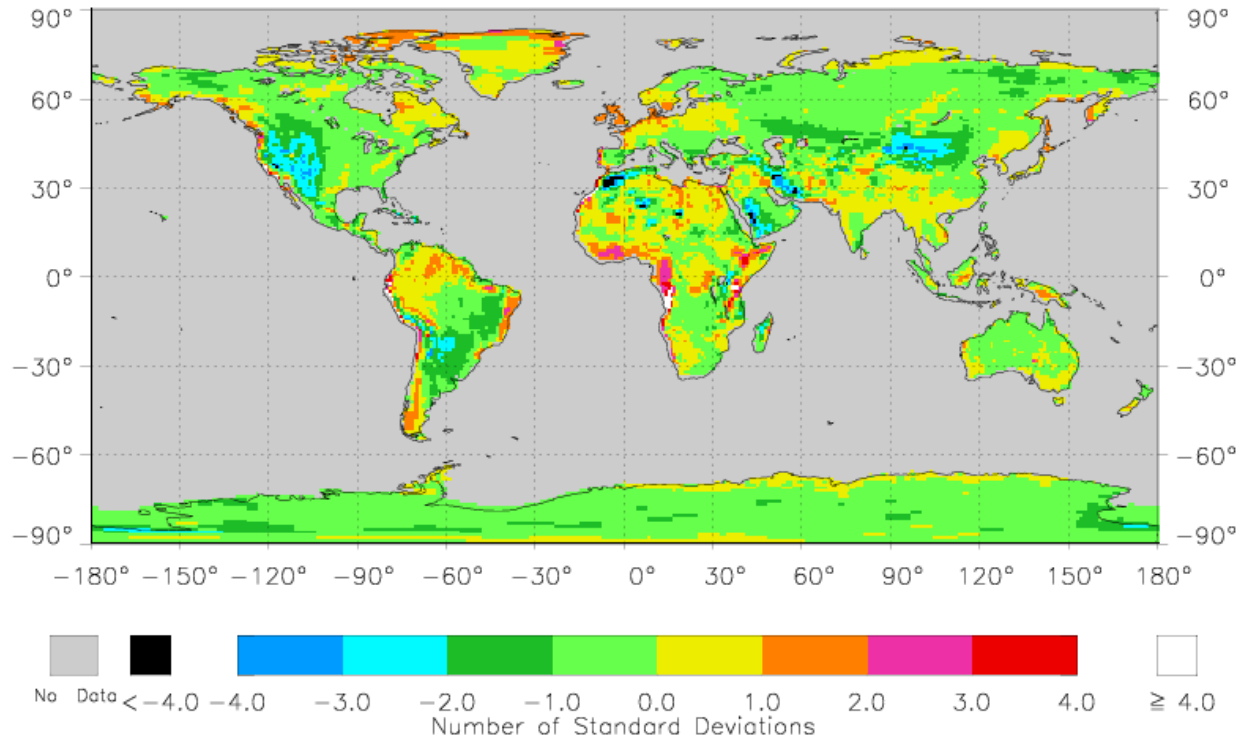

Figure 8. Map of empirical orthogonal functions of cloud forcing of downward longwave flux over land for a) EOF-1 b) EOF-2.

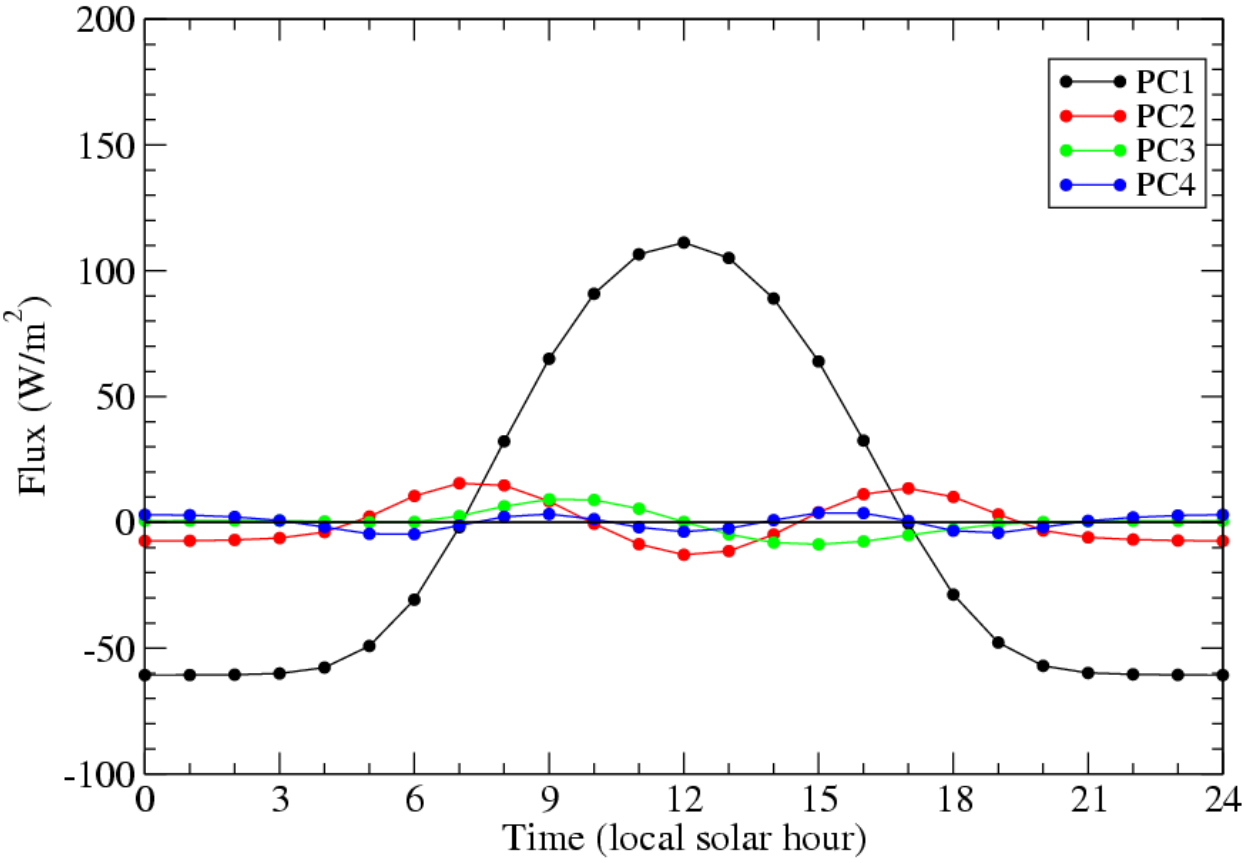

Figure 9. Principal components of diurnal cycles of cloud forcing of downward shortwave flux over ocean.

a)

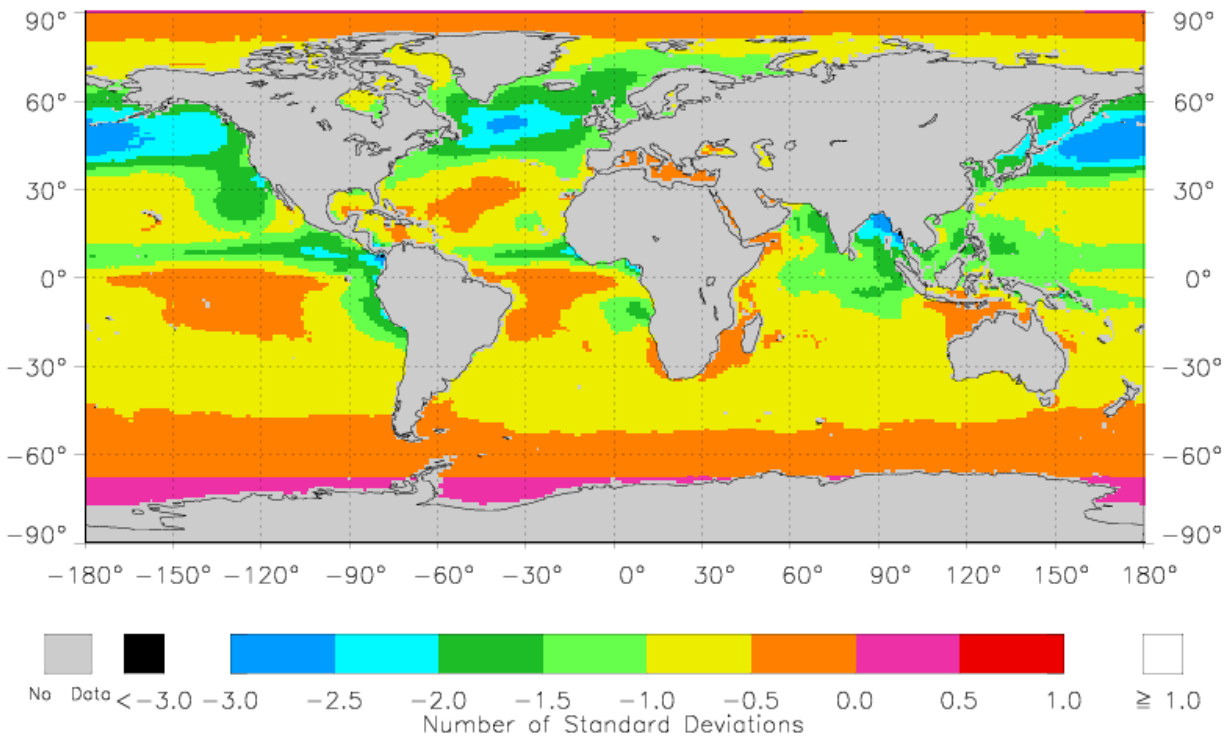

b)

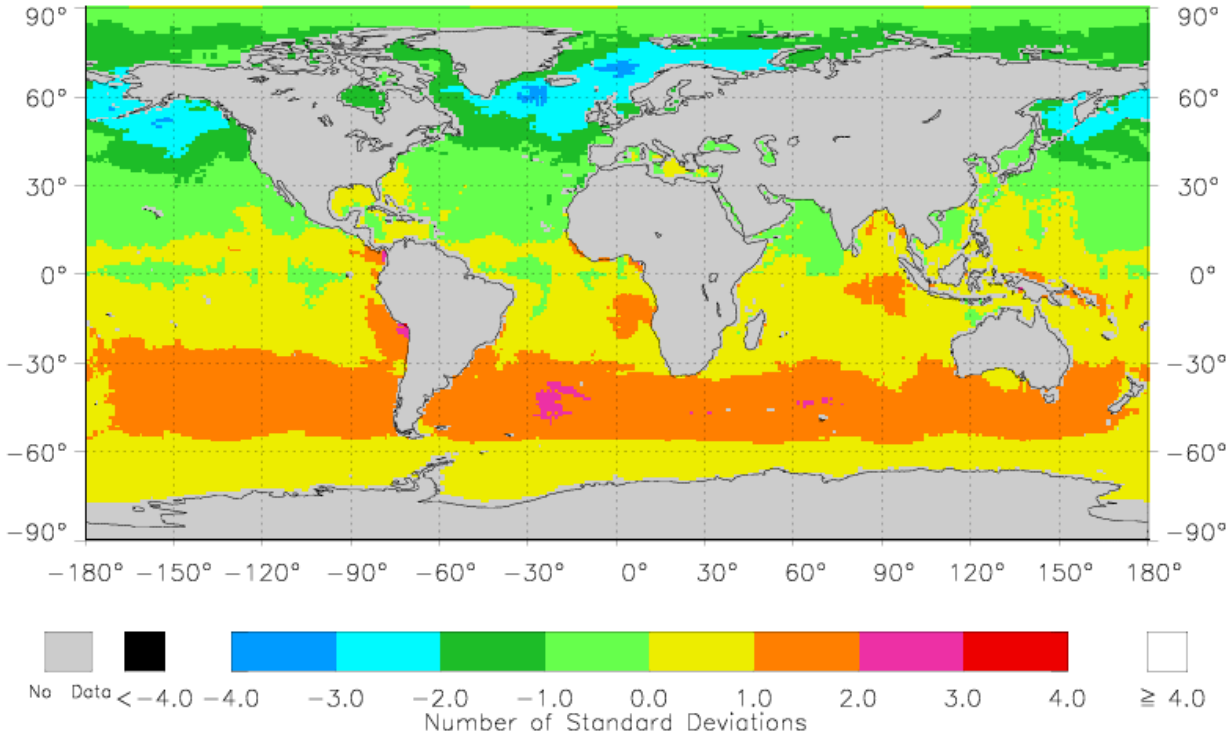

Figure 10. Map of empirical orthogonal functions of cloud forcing of downward shortwave flux over ocean for a) EOF-1 b) EOF-2.